Stage-dependent dynamics and modulation of spontaneous waves in the developing rabbit retina

Mohsin Md. Syed, Seunghoon Lee, Jijian Zheng and Z. Jimmy Zhou

Departments of Physiology and Biophysics and Ophthalmology, University of Arkansas for Medical Sciences, Little Rock, AR 72205, USA

We report here a systematic investigation of the dynamics, regulation and distribution of spontaneous waves in the rabbit retina during the course of wave development prior to eye opening. Three major findings were obtained in this longitudinal study. (1) Spontaneous retinal waves underwent three developmental stages, each of which displayed distinct wave dynamics, pharmacology and mechanism of generation and regulation. Stage I waves emerged prior to synaptogenesis and appeared as frequent, fast propagating waves that did not form spatial boundaries between waves. These waves could be inhibited by blockers of gap junctions and adenosine receptors, but not by nicotinic antagonists. Stage I waves lasted about one day (around embryonic day 22) and then switched rapidly to stage II, resulting in slower and less frequent waves that could be blocked by nicotinic antagonists and had a characteristic postwave refractory period and spatial boundaries between adjacent waves. Immediately after the transition from stage I to stage II, the waves could be reverted back to stage I by blocking nicotinic receptors, indicating the presence of mutually compensatory mechanisms for wave generation. Stage III waves emerged around postnatal day 3–4 (P3–4), and they were mediated by glutamtergic and muscarinic interactions. With age, these waves became weaker, more localized and less frequent. Spontaneous waves were rarely detected after P7. (2) GABA strongly modulated the wave dynamics in a stage- and receptor type-dependent manner. At stage I, endogenous $GABA_B$ activation downregulated the waves. The $GABA_B$ modulation disappeared during stage II and was replaced by a strong $GABA_{A/C}$-mediated inhibition at stage III. Blocking $GABA_{A/C}$ receptors not only dramatically enhanced spontaneous stage III waves, but also induced propagating waves in >P7 retinas that did not show spontaneous waves, indicating a role of GABA inhibition in the disappearance of spontaneous waves. (3) Spontaneous retinal waves were found in both the inner and outer retina at all three stages. The waves in the outer retina (ventricular zone) also showed stage-dependent pharmacology and dynamics. Together, the results revealed a multistaged developmental sequence and stage-dependent dynamics, pharmacology and regulation of spontaneous retinal waves in the mammalian retina. The presence of retinal waves during multiple developmental stages and in multiple retinal layers suggests that the waves are a general developmental phenomenon with diverse functions.

(Received 14 April 2004; accepted after revision 6 August 2004; first published online 12 August 2004)
Corresponding author Z. J. Zhou: Department of Physiology and Biophysics, University of Arkansas for Medical Sciences, 4301 W. Markham Street, Mail Slot 505, Little Rock, AR 72205-7199, USA. Email: zhoujimmy@uams.edu

Spontaneous waves of excitation in the developing mammalian retina (Masland, 1977; Maffei & Galli-Resta, 1990; Meister *et al.* 1991) are believed to play an important role in activity-dependent visual development (Katz & Shatz, 1996), particularly the refinement of eye-specific layers in the dorsal lateral geniculate nucleus (dLGN) (Penn *et al.* 1998; Stellwagen & Shatz, 2002; Grubb *et al.* 2003) and retinotopic maps in the superior colliculus (McLaughlin *et al.* 2003), although the exact function of the waves in retinogenicular development remains controversial (Huberman *et al.* 2003). Recent studies have demonstrated that retinal waves exist during an extensive developmental period (Bansal *et al.* 2000; Wong *et al.* 2000; Zhou & Zhao, 2000; Demas *et al.* 2003), well beyond the critical period for eye-specific layer formation in the dLGN (Robinson, 1991), suggesting that the waves may play different roles at different developmental stages. Rhythmic Ca^{2+} transients and propagating Ca^{2+} waves have also been found in the ventricular zone (VZ) of the retina (Catsicas *et al.* 1998;

 DOI: 10.1113/jphysiol.2004.066597

Zhou *et al.* 2002; Syed *et al.* 2004), indicating a likely role of spontaneous retinal activity in the early development of the retina itself (Pearson *et al.* 2002).

To understand the potentially diverse functions of retinal waves at various stages of development, it is important to determine the sequence of wave development itself. Although retinal waves have been studied extensively in a variety of species (Feller, 1999; Wong, 1999), little is known about the entire developmental course of retinal waves. It has remained unclear how the waves initiate, progress and disappear during development, and what mechanisms regulate the wave dynamics at various developmental stages. Spontaneous waves in the inner mammalian retina were previously known to develop through two pharmacological stages: an early stage wave mediated mainly by nicotinic interactions, and a late stage wave driven by glutamatergic (Feller *et al.* 1996; Zhou, 1998; Bansal *et al.* 2000; Wong *et al.* 2000; Zhou & Zhao, 2000) and muscarinic (Zhou & Zhao, 2000) systems. More recently, an even earlier stage was reported in embryonic mice, during which some, but not all, waves are resistant to nicotinic antagonists (Bansal *et al.* 2000). However, it is unknown what mediates this early, nicotinic receptor-independent activity.

As development proceeds, changes in retinal wave dynamics have been found in a number of species (Wong & Oakley, 1996; Bansal *et al.* 2000; Demas *et al.* 2003; Sernagor *et al.* 2003*b*), consistent with the idea that the changing wave pattern may encode changing cues for visual development. The wave dynamics have also been shown to be modulated by cAMP in the ferret (Stellwagen *et al.* 1999; Bansal *et al.* 2000) and mouse (Bansal *et al.* 2000), by $GABA_A$ interaction in the turtle (Sernagor *et al.* 2003*b*), and by $GABA_B$ activation in the chick (Catsicas & Mobbs, 2001). However, it is unclear how the wave pattern in any one species changes systematically over the entire course of wave development, and whether the regulatory mechanisms shape wave dynamics differently at different stages of development.

This study systematically investigated the dynamics, regulation and distribution of spontaneous waves in the rabbit retina, starting from the first appearance of the wave prior to synaptogenesis, to the last stage of the wave shortly before eye opening. The results provided a comprehensive view of the developmental process of spontaneous waves in the mammalian retina. Preliminary results of this study have been reported in abstract form (Zhao *et al.* 1999; Zhou *et al.* 2002).

Methods

Calcium imaging and patch-clamp recording in the flatmount rabbit retina

Retinal flatmounts were prepared from New Zealand White and New Zealand Red rabbits aged between embryonic day 20 (E20, gestation period = 31 days) and postnatal day 14 (P14) as previously described (Zhou, 1998; Zhou & Zhao, 2000). Embryonic rabbits were delivered by Caesarian section from pregnant rabbits (4–5 kg in weight), which were deeply anaesthetized with 1–2 ml of pre-mixed (at a ratio of 100 : 8) ketamine (100 mg ml^{-1}) and xylazine (100 mg ml^{-1}) (I.V) during the surgery. After Caesarian section, the doe was killed immediately with an overdose of sodium pentobarbital (250 mg, I.V.). All procedures involving the use of animals were in accordance with the National Institutes of Health guidelines as implemented by the institutional animal care and use committee. Immediately after an animal was killed by an overdose of sodium pentobarbital, retinas were dissected in cold (~10°C) Hepes-buffered Ames medium, which was modified from Ames medium (Ames & Nesbett, 1981) by replacing $NaHCO_3$ with 20 mM Hepes. Isolated retinas were cut into ~3 × 5 mm pieces and mounted on black filter paper (HABP, Millipore, Bedford, MA, USA) with either the vitreal or ventriclar surface facing the paper, depending on the experimental requirement.

To load the calcium indicator dye Fura-2AM (Molecular Probes, Eugene, OR, USA), retinal flatmounts were incubated in Hepes-buffered Ames medium containing 10 μM Fura-2AM and 0.001% pluronic acid for 1–6 h at 30°C. The extracellular matrix and immature Müller cell endfeet that covered ganglion cells were partially removed with forceps, so that ganglion and displaced amacrine cells could be loaded with the dye nearly uniformly in local areas ($> 4\ mm^2$) of the retina up to age P7–8. Loading of Fura-2AM in the distal (ventricular) surface of the retina was also nearly uniform at all ages tested (E20–P8). During Ca^{2+} imaging, the recording chamber was continuously superfused (3–4 ml min^{-1}) with Ames medium at 35–37°C. Cells in the ganglion cell layer were imaged with an intensified, cooled CCD camera (I-Pantamax, Roper Scientific Instruments, Princeton, NJ, USA) mounted on a fixed-stage, upright microscope (Olympus BX50WI, Olympus USA, New York).

Whole-cell patch-clamp recordings were made from ganglion cells in the flatmount retina (without filter paper) as previously described (Zhou, 1998). Simultaneous patch-clamp and Ca^{2+} imaging was made from Fura-2AM-loaded retina under a 40× water immersion objective lens (NA = 0.8) (Zhou, 2001). The voltage and current traces were digitized at 10 kHz and stored on computer hard drive via Power Laboratory (AD Instruments, Colorado Spring, CO, USA) and subsequently filtered (Gaussian digital) and redigitized at lower rates depending on the resolution required. The images were acquired at a rate of one frame per second, with an exposure (integration) time of 0.6 s. The presence of a dye-free patch pipette in the field of view did not interfere with fluorescence imaging of retinal waves. The pipette resistance was 5–7 MΩ measured in Ames

medium and a standard pipette solution containing (mM) 95 K-gluconate, 15 KCl, 5 NaOH, 0.5 $CaCl_2$, 2 $MgCl_2$, 5 EGTA, 2 ATP, 0.5 GTP, 2 ascorbic acid and 10 Hepes. Drugs were applied to the retina by bath perfusion (dead volume: ~2 ml). Ames and Hepes-buffered Ames media were saturated with carbogen (95% O_2, 5% CO_2) and oxygen, respectively. All pharmacological agents used in this study were purchased from Sigma Chemicals (St Louis, MO, USA) except CGP55845 and baclofen, which were purchased from Tocris Cookson (Bristol, UK).

Data acquisition and analysis

Fluorescence images of the retina were collected and analysed with the software Axon Imaging Workbench (AIW, Axon Instruments, Union City, CA, USA) and MetaImaging (MetaFluor and MetaMorph, Universal Imaging Inc., Downing, PA, USA) software. To monitor the excitability of the retina, oval zones were drawn in various regions of the image field. The average fluorescence intensity in each zone was plotted as a function of time $F(t)$. The relative change in the emission fluorescence intensity ($\triangle F/F$) was defined as $[F(t) - F_o(t)]/F_o(t)$, where $F_o(t)$ was the baseline intensity, which was obtained by drawing a curve that connected the fluorescence intensity values in the absence of waves. For simplicity, $\triangle F/F$ from a single zone, selected randomly from the field of view, was shown in most figures, but similar results were also found from most of the remaining zones in the field. Thus, the measured $\triangle F/F$ from a single zone not only reflected the Ca^{2+} activities in the zone, but also indicated the presence of a wave that passed through the zone. This was also verified by measuring $F(t)$ in a selected zone with the software, while playing back the images in a movie series, so that the appearance of the waves could be observed simultaneously with the occurrence of $\triangle F(t)$ measured from the zone. The propagation of retinal waves was imaged with a 10 × objective lens (NA = 0.3) at an acquisition rate of one frame per 0.9 s (with an exposure time of 0.6 s). Differential images ($\triangle F$) of the wave were obtained by subtracting a control image (averaged from four frames recorded immediately before a wave) from images recorded during the wave. To measure the speed (v) of the wave, the rate of displacement of the wavefront in the direction of wave propagation was measured using MetaMorph. Data were expressed as mean ± S.D. Student's t test was used to determine the significance of the data.

Results

The earliest propagating wave in the developing rabbit retina

To understand the developmental sequence of spontaneous waves in the mammalian retina, we began by examining the wave property when the waves first appeared in the rabbit retina. Ca^{2+} imaging was made from Fura-2AM-loaded retinas isolated from rabbits starting at age E20, when ganglion cells were differentiated but had not yet undergone chemical synaptogenesis (Greiner & Weidman, 1982). At this age, ganglion cells were quite passive in their membrane electric properties, showing only small voltage-gated currents and very small regenerative potentials (data not shown). No propagating wave of spontaneous activity was found from the ganglion cell layer (GCL) at E20 (6 rabbits) and E21 (5 rabbits). The earliest age at which spontaneous waves were detected was E22, when ganglion cells began to generate large action potentials. E22 was also the age when ganglion cell axons first reached their central visual targets (Crabtree, 1990), suggesting that the earliest electric signals from the retina to the central visual targets were in the form of propagating waves. Figure 1 shows an example of patch-clamp recording from a ganglion cell and simultaneous Ca^{2+} imaging from the area surrounding the patch-clamped cell in a Fura-2AM-loaded E22 retina. The rhythmic bursts of spikes in the ganglion cell were found to correlate with the Ca^{2+} rises measured from the surrounding area (Fig. 1, $n = 3$). Importantly, at E22 neither the bursts of spikes in individual ganglion cells, nor the propagating Ca^{2+} waves in the GCL were sensitive to most neurotransmitter receptor antagonists, including blockers of acetylcholine (both nicotinic and muscarinic) receptors, ionotropic glutamate and GABA receptors and glycine receptors (Figs 1 and 2*A*, $n = 6$), suggesting that the earliest spontaneous waves were distinctly different from the waves previously reported in older mammalian retinas.

To investigate the mechanism underlying the earliest spontaneous retinal wave, we tested whether signalling via gap junctions was important in generating the waves. As shown in Fig. 2*A*, the gap junction blocker 18β-glycyrrhetinic acid (18β-GA, 75 μM) blocked E22 waves completely ($n = 3$), while a cocktail of hexamethonium, atropine, 6-cyano-7-nitroquinoxaline-2,3-dione (CNQX), AP7, picrotoxin and strychnine failed to block the waves. Thus, gap junction communication plays a crucial role in the propagation of the earliest spontaneous retinal waves in rabbits (see below).

We next examined whether adenosine played a role in spontaneous wave formation at E22. Application of the broad-band adenosine receptor antagonist aminophylline (100–500 μM) completely and reversibly blocked the earliest wave (Fig. 2*B*, $n = 4$). Because adenosine has been reported to up-modulate retinal waves via the cyclic AMP pathway in older (postnatal) ferrets and mice (Stellwagen *et al.* 1999; Bansal *et al.* 2000), we also tested the effect of the adenylate cyclase activator, forskolin. Application of forskolin (10 μM, $n = 3$) increased the

wave frequency tremendously (Fig. 2*C*). In the presence of forskolin, the waves rapidly propagated across the field of view one immediately after another, and the Ca^{2+} concentration in ganglion cells underwent continuous oscillation (Fig. 2*C*). Thus, the dynamics of the earliest retinal wave in rabbits were regulated strongly by the cyclic AMP pathway. In contrast, depleting intracellular Ca^{2+} stores with thapsigargin (2 μM, $n = 2$) did not block the wave (Fig. 2*D*), even though thapsigargin caused a large, transient increase in the baseline Ca^{2+} level, presumably due to the blockade of Ca^{2+} uptake into intracellular stores, suggesting that the earliest retinal wave was not generated by Ca^{2+} release from thapsigargin-sensitive intracellular Ca^{2+} stores.

In addition to adenosine receptor antagonists, the common purinergic receptor antagonist reactive blue-2

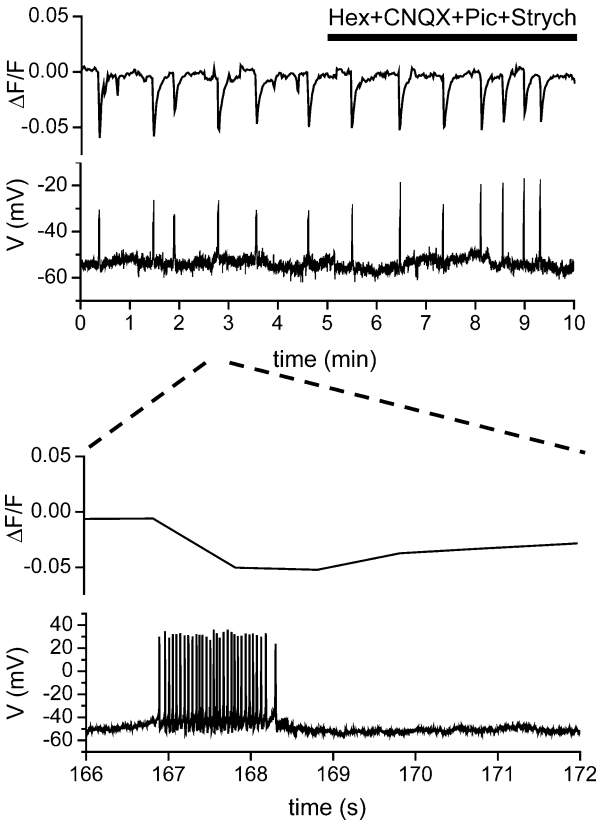

Figure 1. The earliest spontaneous waves in the developing rabbit retina
Simultaneous Ca^{2+} imaging and patch-clamp recording in the ganglion cell layer of an E22 rabbit retina loaded with Fura-2AM. Relative changes in fluorescence intensity ($\Delta F/F$) were averaged from the entire field of view (270 μm × 270 μm) under a 40× objective lens (top trace), showing rhythmic Ca^{2+} transients (downward deflections) appearing in synchrony with bursts of spikes (*V*) recorded from a current-clamped ganglion cell in the same field of view (the second trace, filtered and digitized at 20 and 50 Hz, respectively). Neither the Ca^{2+} transients, nor the spikes were blocked by a cocktail of common neurotransmitter receptor blockers, including 100 μM hexamethonium (Hex), 35 μM CNQX, 100 μM picrotoxin (Pic) and 4 μM strychnine (Strych). The third (filtered and digitized at 1 and 2 kHz, respectively) and fourth traces show an expanded view of a portion of the voltage trace and fluorescence changes, respectively. The fluorescence changes appeared to lead the spikes because the wave, which entered the field of view from outside of the frame, reached the area of imaging (the entire frame) before it reached the cell under patch clamp.

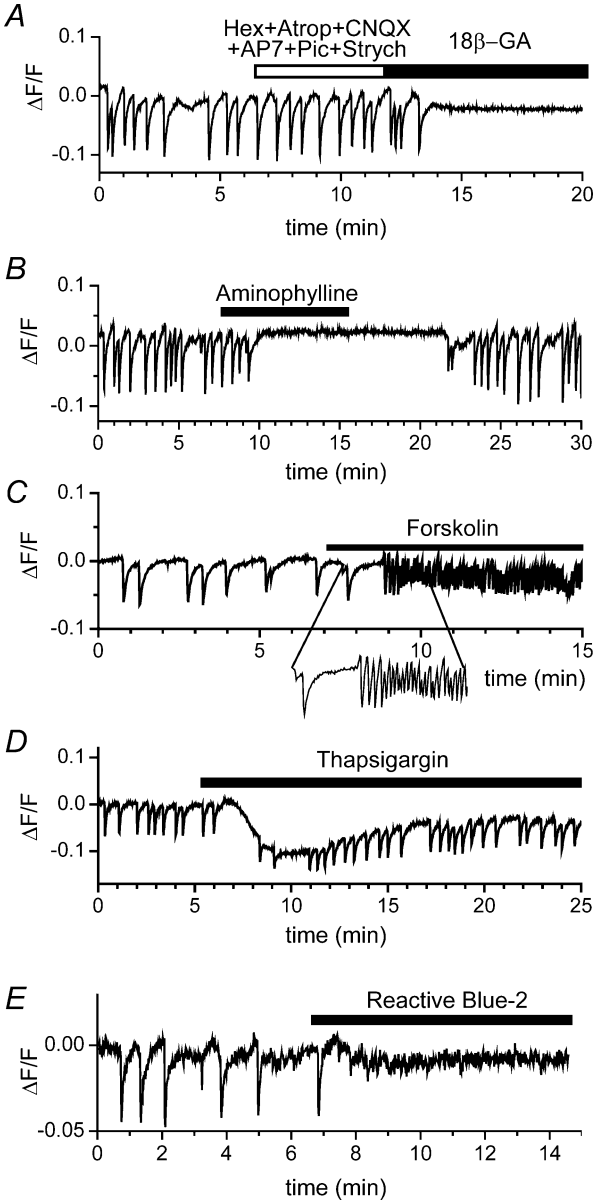

Figure 2. Pharmacology of the earliest spontaneous Ca^{2+} waves in the ganglion cell layer of E22 rabbits
A, the waves (downward deflections in $\Delta F/F$) were not affected by a cocktail of antagonists, containing hexamethonium (Hex, 100 μM), atropine (2 μM), CNQX (50 μM), D-AP7 (100 μM), picrotoxin (100 μM) and strychnine (8 μM), but they were completely blocked by the gap junction blocker 18β-GA (75 μM). *B*, the spontaneous waves were also reversibly blocked by the adenosine receptor antagonist, aminophylline (500 μM). *C*, forskolin (1 μM) dramatically increased the frequency of spontaneous waves. *D*, blocking Ca^{2+} uptake into intracellular Ca^{2+} stores with thapsigargin (1 μM) produced a large transient increase in intracellular Ca^{2+}, but did not block the rhythmic spontaneous Ca^{2+} waves. *E*, the purinergic receptor blocker, reactive blue-2 (50 μM), also completely blocked the spontaneous waves.

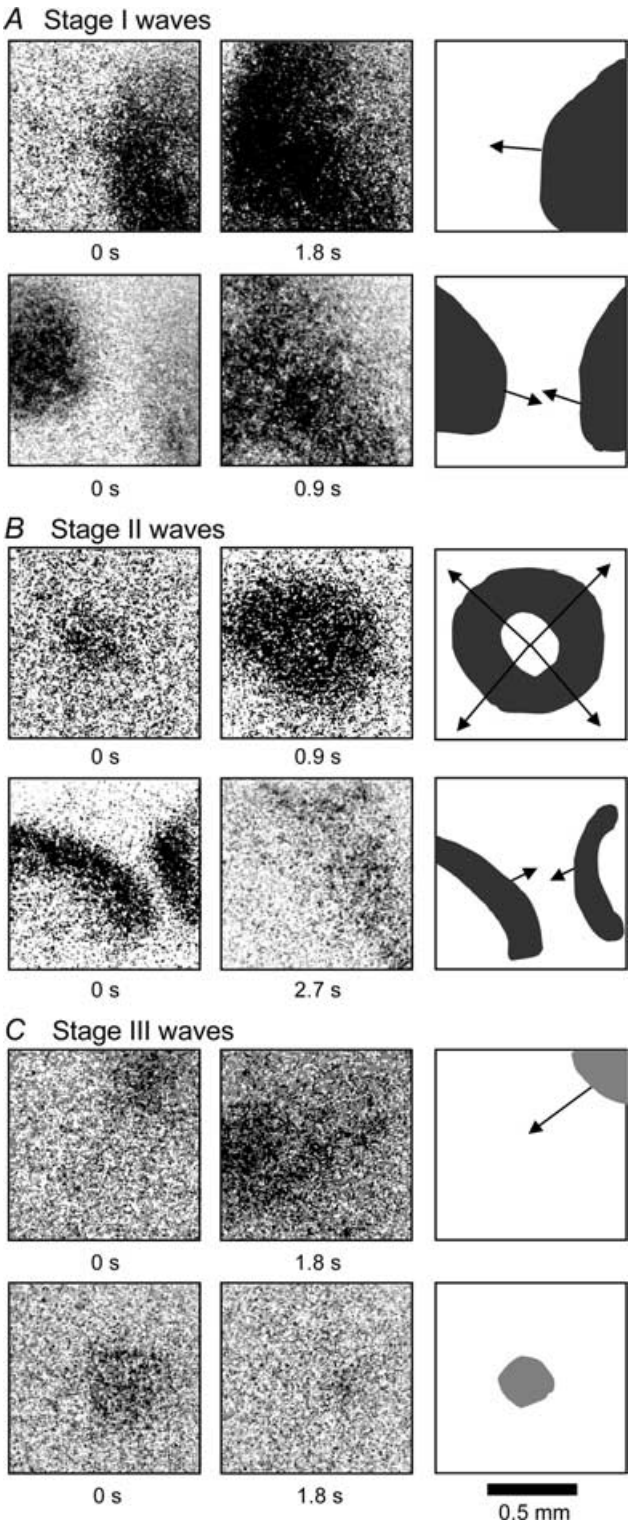

Figure 3. Stage-dependent wave dynamics in the ganglion cell layer (GCL)
Difference images (ΔF) were taken from Fura-2AM-loaded GCL at three developmental stages. The dark areas indicate regions of elevated intracellular Ca^{2+} associated with the wave. Each row shows two image frames of the same wave(s) together with a cartoon (right) depicting the propagation pattern of the wave(s). *A*, a stage I (E22) wave with a large wavefront and fast lateral propagation (upper row). When two stage I (E22) waves collided, they superimposed and passed through each other (lower row). *B*, a stage II (E29) wave propagating as a two-dimensional plane wave (upper row). When two stage II (E29) waves collided, they annihilated each other (lower row). *C*, stage III waves (P5) were weaker (smaller $\Delta F/F$, also shown qualitatively in a lighter shade of grey in the cartoon) compared to other two stages. They sometimes showed clear lateral propagation (upper row), but most of the time appeared as a local burst of Ca^{2+} increases without clear lateral propagation (lower row). Movies showing the propagation of the waves in *A* (upper), *B* (upper) and *C* (lower) are provided in the Supplementary materials.

(30–100 μM) also effectively blocked the waves in E22 rabbits (Fig. 2*E*) ($n = 3$), raising the possibility of an involvement of purinergic receptor activation in the waves. Suramin, a different purinergic antagonist, also blocked the wave, but only at a high concentration (500 μM, $n = 2$). However, another common purinergic antagonist, pyridoxal-5′-phosphate-6-phenylazo-2′,4′-disulphonate (PPADS, 100–800 μM), did not have a consistent effect ($n = 4$), even though PPADS could block ATP-activated currents in ganglion cells (data not shown). The different effects of these antagonists on the wave might be attributable to the fact that different subclasses of P2X and P2Y receptors have very different sensitivities to various purinergic antagonists (Burnstock & Williams, 2000; Norenberg & Illes, 2000; von Kugelgen & Wetter, 2000). On the other hand, we could not rule out the possibility that the blockade of the wave by reactive blue-2 and suramin could be a result of a non-specific effect of the drugs, because attempts to exhaust endogenous ATP with hexokinase (3–10 u/ml) failed to block the wave ($n = 3$). The possibility of a purinergic involvement in retinal wave generation or regulation remains to be further investigated.

Spontaneous retinal waves in rabbit developed through three distinct stages

The unique pharmacological profile of the spontaneous wave in E22 rabbits suggested that the waves prior to synaptogenesis were generated by a distinct mechanism. Based on this finding and on the pharmacological properties of retinal waves previously described in older rabbits (Zhou & Zhao, 2000), we classified spontaneous waves in the inner rabbit retina into three stages. Stage I waves appeared between E22 and E23. They were not mediated by the common fast neurotransmitter receptors, including acetylcholine, glutamate, GABA and glycine receptors; however, they were abolished by the blockers of gap junctions, adenosine receptors, and possibly, purinergic receptors. Stage II waves occurred between E24 and P1, when the nicotinic system was the primary driving force for the waves (Zhou & Zhao, 2000). Stage III waves emerged at ~P4, after a transitional period (P2–P3) during

which the excitatory drive for the wave switched from a nicotinic system to a system involving both glutamate and muscarinic receptors (Zhou & Zhao, 2000). Stage III waves were found between P4 and P8, the oldest age studied with Ca^{2+} imaging. Movies showing examples of stage I–III waves are provided in the Supplementary Materials.

Stage I waves. Stage I waves appeared in the inner retina prior to synaptogenesis. These waves were very strong, sweeping across the entire field of view (1.15 × 1.15 mm) (Fig. 3*A*, upper) at an average speed of $451 \pm 92\ \mu m\ s^{-1}$ ($n = 20$), much faster than the waves at stages II and III (Fig. 5*B*). Stage I waves also appeared frequently, with an average interwave interval of 36 ± 18 s ($n = 68$) (Fig. 5*B*). The distribution of the interwave interval (Fig. 4*C*) showed a minimum interval of ≤5 s, indicating a lack of prolonged postwave refractory period. Consequently, stage I waves did not form a clear boundary between neighbouring waves. When two waves collided, they superimposed (Fig. 3*A*, lower), instead of annihilating each other. Figure 4*A* shows, in the same retinal area, two successive waves that were separated by only 8 s. The Ca^{2+} increases during these two waves (measured as $\Delta F/F$ from the small circles shown in Fig. 4*A*, upper) were additive (Fig. 4*B*, arrows), indicating a superposition of the two waves. This propagation pattern sharply contrasted the wave patterns in the other two stages (see below).

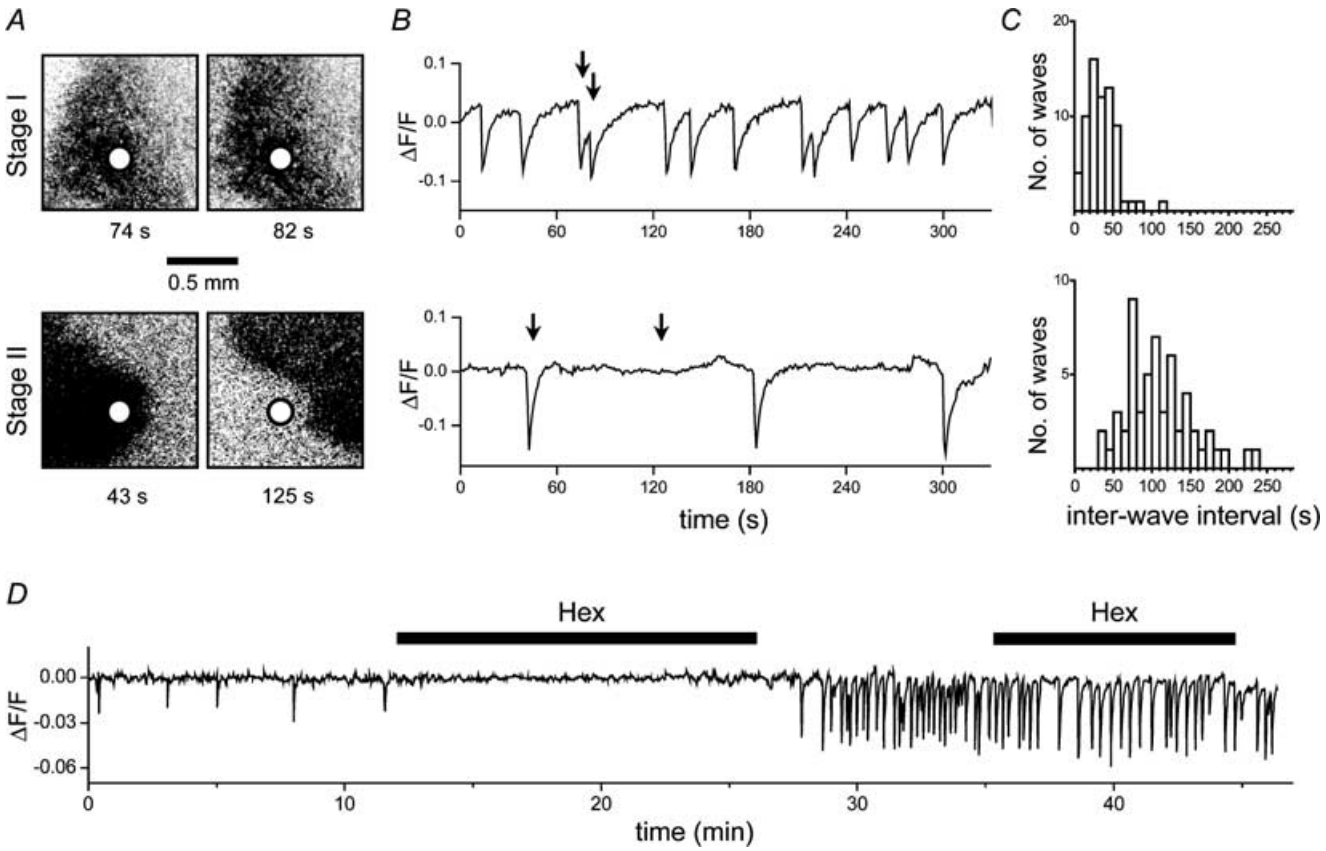

Figure 4. Comparison and transition between stage I and stage II waves
A, difference images (ΔF) of two consecutive stage I waves (upper) and two consecutive stage II waves (lower), showing the spatial coverage of each wave. The two stage I waves originated in the same area within 8 s, and they superimposed on one another without a boundary between them (upper row). The two stage II waves were separated by 82 s, yet still formed a clear boundary between them. *B*, relative fluorescence changes ($\Delta F/F$) measured as a function of time from the small white circular regions indicated in *A*. The stage I waves (upper) were very frequent and showed intensity changes ($\Delta F/F$) that were additive between the closely successive waves. Stage II waves (lower) had a long refractory period and obeyed clear spatial boundaries, resulting in a much longer interwave interval. Arrows indicate times when the images in *A* were taken. *C*, distributions of interwave intervals at stage I (upper) and stage II (lower), showing a minimum interwave interval of <5 s at stage I and 35 s at stage II. Waves that did not reach the central circle, such as the one at 82 s, were not counted in the calculation of interwave interval. The bin width in the histograms is 5 s. *D*, blocking stage II waves in the ganglion cell layer of an E22 retina with hexamethonium (Hex, 150 μM) induced the reappearance of stage I waves in the same retinal area. Application of Hex (150 μM) for the second time did not block the stage I waves.

Stage II waves. The second stage of spontaneous waves in rabbits began at E24, when the inner plexiform layer (IPL) formed by neuronal processes containing microtubules and vesicles first appeared (Greiner & Weidman, 1982), indicating the onset of early conventional synaptogenesis in the IPL. Pharmacologically, stage II waves (E24–P1) differed dramatically from stage I waves, because they could be readily blocked by nicotinic antagonists (Zhou & Zhao, 2000). The transition from stage I to stage II occurred around E23, when the nicotinic system emerged as the major excitatory drive for the wave (occasionally, one or two from a litter of seven to nine E22 pups would show stage II wave pharmacology in the area of the retina being studied, perhaps as a result of developmental variations and/or developmental gradients within the retina). The wave dynamics also underwent a drastic transition from stage I to stage II (Fig. 4*A*–*C*). Although stage II waves remained robust and propagating (Fig. 3*B*, upper), their speed became significantly slower ($200 \pm 50\ \mu m\ s^{-1}$, $n = 20$) compared to that of stage I waves ($451 \pm 92\ \mu m\ s^{-1}$, $n = 20$), and the interwave interval increased dramatically from 36 ± 18 s at stage I to 113 ± 25 s ($n = 39$) at stage II (Figs 4*C* and 5*B*). The minimum interwave interval at stage II was ~35 s (Fig. 4*C*), indicative of the presence of a long-lasting postwave refractory process (Feller *et al.* 1997). It was at stage II that spatial boundaries became evident between neighbouring waves. When two waves collided, they annihilated each other (Fig. 3*B*, lower), instead of superimposing on one another as in stage I (Fig. 3*A*, lower). Figure 4*A* (lower) shows two consecutive stage II waves separated by as long as 82 s. Yet, the two waves still formed a clear border between them, such that the second wave stopped right at the boundary of the preceding wave.

Interestingly, in an E22 retina, we observed the coexistence of two mechanisms that supported stage I and stage II waves, respectively. As shown in Fig. 4*D*, this piece of retina initially generated typical stage II waves, which occurred at an interwave interval of 2–3 min and could be completely blocked by 150 μM hexamethonium, suggesting the transition from stage I to stage II waves had already completed. Remarkably, soon after blocking these stage II waves with hexamethonium, the same region of the retina began to generate typical stage I waves, which appeared at an interwave interval of less than 20 s and were no longer sensitive to hexamethonium (150 μM). Thus, blocking stage II waves could induce the reappearance of stage I waves during the transitional period. This result is consistent with our finding that the transition between stages I and II waves occurred abruptly (between E22 and E23), perhaps by a switch between two different mechanisms of wave generation.

Stage III waves. The emergence of stage III waves in the rabbit began as retinal development progressed beyond the early stage of conventional synaptogenesis, when vesicular glutamate transporters began to appear in the mammalian IPL (Johnson *et al.* 2003) and early ribbon synaptogenesis in IPL was just about to occur (McArdle *et al.* 1977). During this period (P4–P8), the waves were insensitive to nicotinic antagonists, but were dependent on

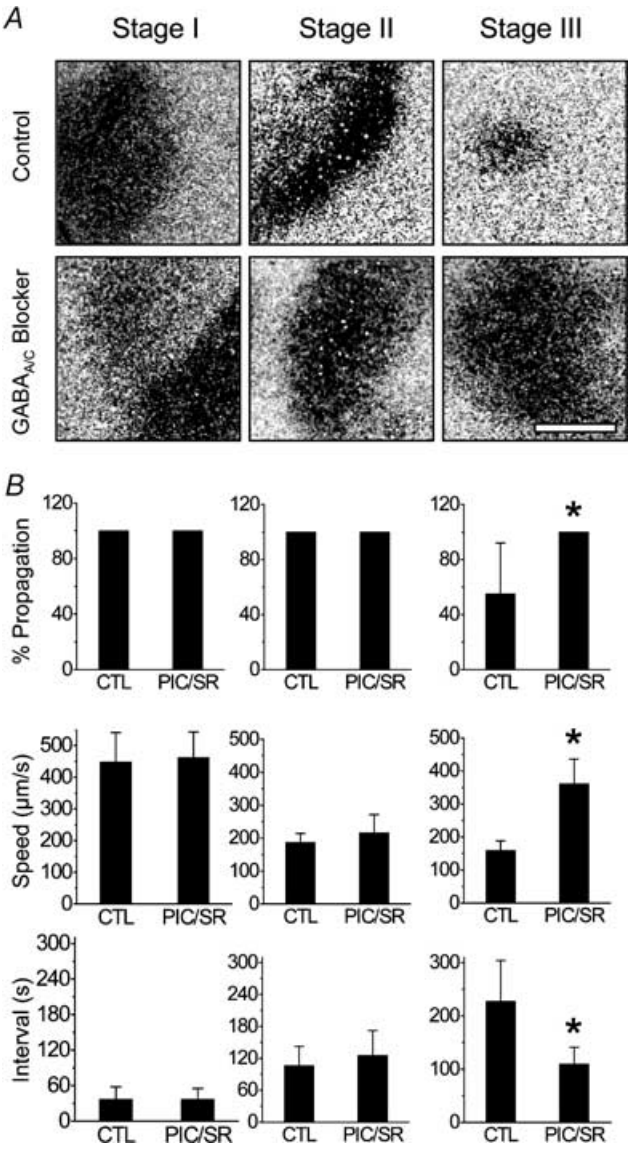

Figure 5. Stage-dependent GABA$_{A/C}$ modulation of inner retinal wave dynamics
A, difference (ΔF) images of typical examples of stage I, II and III waves recorded under the control condition (upper row) and in the presence of 100 μM picrotoxin (lower row). Picrotoxin had no clear effect on stages I and II waves, but dramatically enhanced stage III waves. These images were selected to show the wavefront size typically seen under each recording condition. Scale bar: 0.5 mm. *B*, summary of the stage-dependent effects of GABA$_{A/C}$ antagonists (100 μM picrotoxin (PIC), or 100 μM SR95531 (SR)) on the percentage of waves that propagated, the wavefront speed and the interwave interval. Asterisks indicate values that are significantly ($P < 0.012$) different between control (CTL) and Pic/SR95331.

glutamatergic and muscarinic drives (Zhou & Zhao, 2000). The transition from stage II to stage III took 2–3 days (P2–P3), during which the emergence of glutamate and muscarinic drives was quite rapid (between P1 and P2), whereas the disappearance of the nicotinic drive took place from P1 to P3/P4. Compared to stage I and stage II waves, spontaneous waves at stage III appeared at a much lower frequency. The average interwave interval reached 228 ± 77 s ($n = 10$) at stage III, up from 36 ± 18 s and 113 ± 25 s ($n = 39$) at stages I and II, respectively (Fig. 5*B*). Many (~45%, Fig. 5) stage III waves did not propagate or propagated only a very short distance before dying out (Fig. 5*B*); they appeared as localized, non-propagating bursts. The amplitude of the Ca^{2+} rise during a wave ($\triangle F/F$) also became progressively smaller after P4, often making it difficult to detect spontaneous stage III waves. Because of the small amplitude and limited lateral propagation of stage III waves, a quantitative measurement of the wave speed was difficult. The average wave speed of a selection of 12 strong and propagating stage III waves was $159 \pm 29\ \mu m\ s^{-1}$.

Notably, we found the progressive weakening of the spontaneous stage III wave with age was associated with the maturation of the GABAergic and glycinergic systems, because picrotoxin and strychnine were very effective in enhancing stage III waves, dramatically increasing the wave frequency and transforming localized bursts of Ca^{2+} into large propagating Ca^{2+} waves (Fig. 5). This result suggests a possible role of the inhibitory GABAergic and glycinergic systems in the progressive weakening and final disappearance of stage III spontaneous retinal waves around the time of eye opening (P11) (see below).

Stage-dependent GABAergic regulation of wave dynamics

$GABA_{A/C}$. To determine whether, in addition to adenosine, acetylcholine and glutamate, other neurotransmitters also contributed to the changing dynamics of retinal waves, we investigated the possible involvement of GABA in modulating the spatiotemporal properties of the waves in rabbit. We first examined the effects of ionotropic GABA receptor antagonists on wave dynamics at various developmental stages (Fig. 5). When SR95531 (100 μM) or picrotoxin (100 μM) was applied to the retina to block $GABA_A$ or $GABA_{A/C}$ receptors, respectively, changes in wave dynamics were observed in a stage-dependent manner. At stage I, picrotoxin had no significant effect on any of the wave parameters examined (Fig. 5), including the percentage of waves that were propagating (control: 100%, $n = 40$; picrotoxin/SR95531: 100%, $n = 40$), the wavefront speed (control: $449 \pm 92\ \mu m\ s^{-1}$, $n = 25$; picrotoxin/SR95531: $463 \pm 80\ \mu m\ s^{-1}$, $n = 25$) and the interwave interval (control: 37 ± 21 s, $n = 60$; picrotoxin/SR95531: 37 ± 18 s, $n = 20$) (Fig. 5).

At stage II, ionotropic GABA currents constituted a significant component of the neurotransmitter input to ganglion and starburst amacrine cells during spontaneous waves (S. Lee and Z. J. Zhou, unpublished observation from patch-clamp recordings). However, blocking this component with picrotoxin or SR95531 had no significant effect on the dynamics of stage II waves. As shown in Fig. 5*B*, all (100%) stage II waves were propagating, regardless of whether they were in control conditions ($n = 40$) or in the presence of picrotoxin or SR95531 ($n = 40$). The wavefront speed was $187 \pm 27\ \mu m\ s^{-1}$ ($n = 13$) in control and $216 \pm 55\ \mu m\ s^{-1}$ ($n = 16$) with picrotoxin/SR95531. The interwave interval was also not significantly different: 106 ± 36 s ($n = 18$) in control and 126 ± 46 s ($n = 16$) with picrotoxin/SR95531 (Fig. 5*B*).

In contrast, as the spontaneous waves became weaker, less frequent and more localized during stage III, picrotoxin or SR95531 became increasingly effective in changing the wave dynamics. In the presence of picrotoxin (100 μM), all of the small and non-propagating spontaneous waves, which accounted for about 45% of the rhythmic bursts seen under the control conditions ($n = 10$ retinas), were converted to large and propagating waves (Fig. 5*A*). The average wavefront speed, which became easily measurable in the presence of picrotoxin, was $361 \pm 75\ \mu m\ s^{-1}$ ($n = 15$), much higher than the average speed of the strongest stage III waves in control conditions (159 ± 29, $n = 12$). The interwave interval was reduced from 228 ± 77 s ($n = 20$) in controls to 110 ± 31 s ($n = 20$) in the presence of picrotoxin or SR95331 (Fig. 5*B*). These results demonstrated that endogenous activation of ionotropic GABA receptors modulated the wave dynamics in an age-dependent manner (Fig. 6*B*, *E*, *G* and *H*), exerting a strong inhibitory effect only during stage III. The developmental profile of this ionotropic GABAergic inhibition matched the developmental expression pattern of the K^+–Cl^- cotransporter, KCC2, in the inner mammalian retina (Vu *et al.* 2000), suggesting a progressive inhibition produced by the shifting of the Cl^- equilibrium potential toward a more hyperpolarized potential.

$GABA_B$. In order to find out if $GABA_B$ receptors were also involved in the modulation of wave dynamics in the rabbit, we investigated the effects of the $GABA_B$ agonist baclofen (50 μM) and antagonist CGP55845 (50 μM) at all three stages of wave development (Fig. 6). At stage I, baclofen completely and reversibly blocked the spontaneous wave ($n = 3$), an effect that was eliminated by a high dose of CGP55845 (Fig. 6*A*, $n = 2$). Application of CGP55845 alone increased the frequency of spontaneous waves dramatically ($n = 5$) (Fig. 6*C*), suggesting that $GABA_B$ receptors were endogenously activated during spontaneous waves and played an inhibitory role in

wave generation. At stage II, application of baclofen reduced the frequency of spontaneous waves by 15 ± 13% ($n = 3$), but did not completely block the wave (Fig. 6*D*) ($n = 3$). However, blocking endogenous $GABA_B$ activity with CGP55845 had no significant effect on the wave dynamics ($n = 5$), suggesting that the endogenous $GABA_B$ system no longer played a significant role in modulating the wave dynamics at this stage. As shown in Fig. 6*F* and *G*, CGP55845 also did not have any significant effect on stage III wave dynamics ($n = 4$), indicating a lack of endogenous $GABA_B$ modulation of the wave at this stage. The exogenous $GABA_B$ agonist baclofen could block stage III waves under the control condition, but not when the waves had already been enhanced by picrotoxin (Fig. 6*F–H*) ($n = 2$). These results suggest that the down-regulation of wave dynamics by the endogenous $GABA_B$ system was transient, occurring only at stage I. As the waves progressed to stages II and III, the endogenous $GABA_B$ influence on the wave quickly diminished, even though $GABA_B$ receptors remained functional, presumably to play different functional roles.

Transition from a $GABA_B$- to a $GABA_A$-mediated regulation of wave dynamics

The above results showed that the GABAergic system in the developing rabbit retina played an important and stage-dependent role in modulating the spontaneous

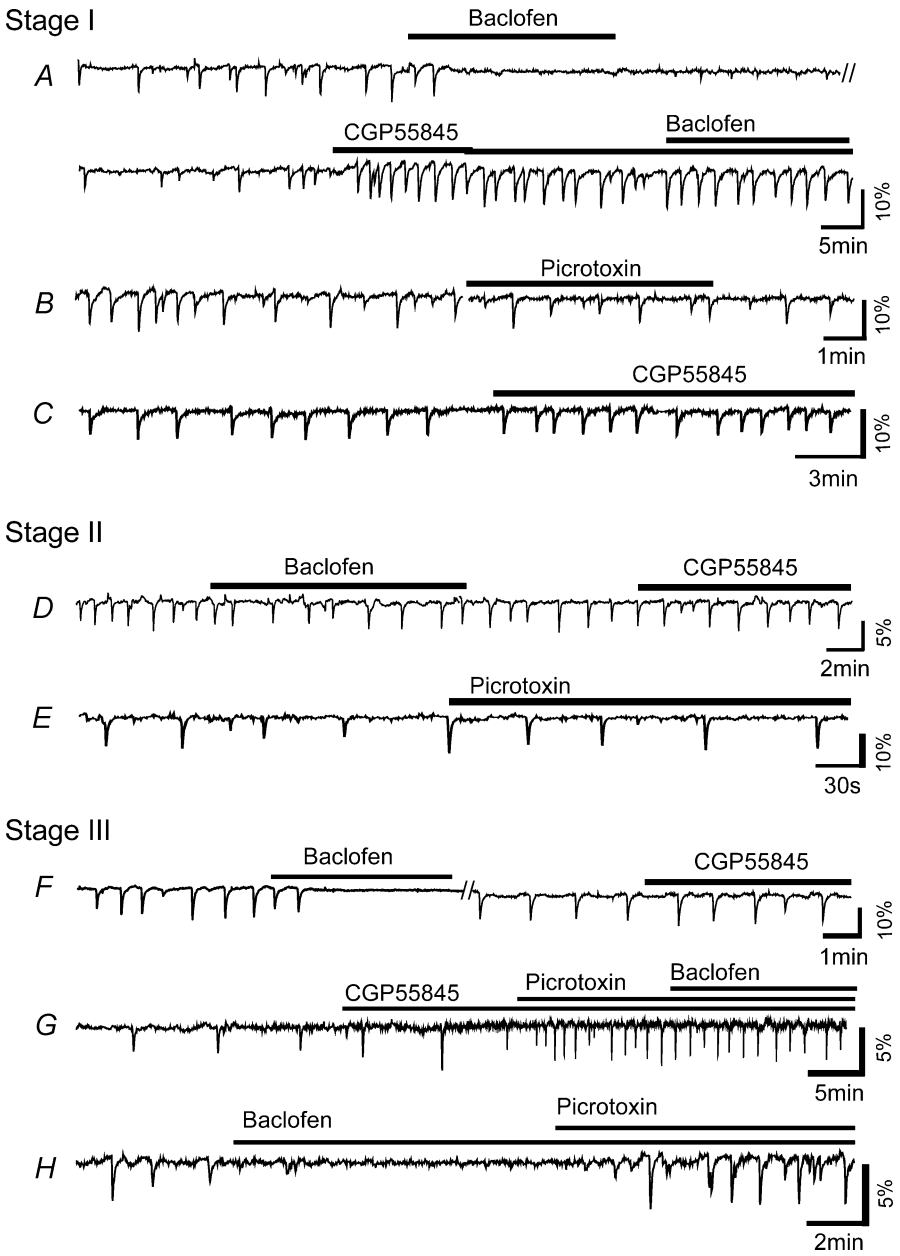

Figure 6. Modulation of wave dynamics by $GABA_{A/C}$ and $GABA_B$ activation
A, activation of $GABA_B$ receptors with baclofen (100 μM) completely and reversibly blocked stage I (E22) spontaneous waves in the ganglion cell layer. The $GABA_B$ antagonist CGP55485 (50 μM) increased the frequency of spontaneous waves at this age and prevented the blocking effect of baclofen. *B*, picrotoxin (100 μM) had no significant effect on wave frequency at stage I. *C*, CGP55485 (50 μM) increased stage I wave frequency in a retina that was never exposed to exogenous $GABA_B$ agonist, confirming the presence of endogenous $GABA_B$ inhibition of spontaneous waves. *D*, at stage II, baclofen (100 μM) only slightly reduced the wave frequency, but CGP55485 (50 μM) did not have any significant effect on the waves, suggesting a lack of endogenous $GABA_B$ modulation of stage II wave frequency. *E*, the $GABA_A$ antagonist, picrotoxin (100 μM), also did not have any significant effect on stage II wave frequency. *F–H*, baclofen (100 μM) blocked the spontaneous wave, but CGP55485 alone had no significant effect on the wave, suggesting a lack of endogenous $GABA_B$ effect on stage III waves. Picrotoxin (100 μM) dramatically increased stage III wave frequency. With the enhancement by picrotoxin, stage III waves were no longer blocked by baclofen (100 μM).

wave dynamics. The overall effect of GABA modulation was to reduce the level of spontaneous activity, through selective activation of two different families of GABA receptors (Fig. 7). During early development (stage I), when the $GABA_A$ system was not yet inhibitory presumably due to a lack of KCC2 expression, the down-modulation of spontaneous retinal waves was mediated by the $GABA_B$ system. At stage II, neither $GABA_A$ nor $GABA_B$ system had a significant effect on the wave dynamics. As the waves progressed to stage III, the $GABA_{A/C}$ system became strongly inhibitory and took over the role of down-regulating the waves, while the $GABA_B$ system no longer participated in the endogenous modulation of the waves. These results revealed a coordinated, stage-dependent GABAergic modulation of retinal waves mediated by a transition from a metabotropic to an ionotropic GABAergic action.

Effects of gap junction blockers

Unlike the changing contributions of various neurotransmitter systems to the spontaneous retinal waves, a contribution of gap junctions to wave generation was implicated at all stages of wave development. The gap junction blocker (18β-GA, 75 μM) was effective in completely blocking spontaneous retinal waves at stages I (Fig. 2*A*, $n = 3$), II (Fig. 8*B*, $n = 6$) and III ($n = 4$). When applied at a low concentration (15 μM), 18β-GA reduced the amplitude and restricted the lateral propagation of stage II waves (Fig. 8*B*), suggesting a dependence of stage II wave propagation on gap junction communication. The inhibitory effects of 18β-GA could also be mimicked by octanol-1 (100 μM, Fig. 8*A*). However, another common gap junction blocker, carbenoxolone (100–200 μM), did not block the waves. The stereoisomer of 18β-GA, 18α-GA, also did not have a significant effect on the waves up to the highest dissolvable concentration of 75 μM ($n = 4$), possibly due to a lack of effective concentration or a lack of sensitivity of the gap junctions involved to this drug. Because of the potential side-effects of gap junction blockers in general, the possibility of a non-specific effect of 18β-GA and octanol-1 on retinal waves cannot be completely ruled out. On the other hand, the very lack of an effect of 18α-GA may serve as a control, arguing against a non-specific effect of 18β-GA on the waves.

Ventricular retinal waves also developed through three pharmacological stages

We previously reported spontaneous waves in the VZ of E24–P0 rabbit retinas (Syed *et al.* 2004). The waves

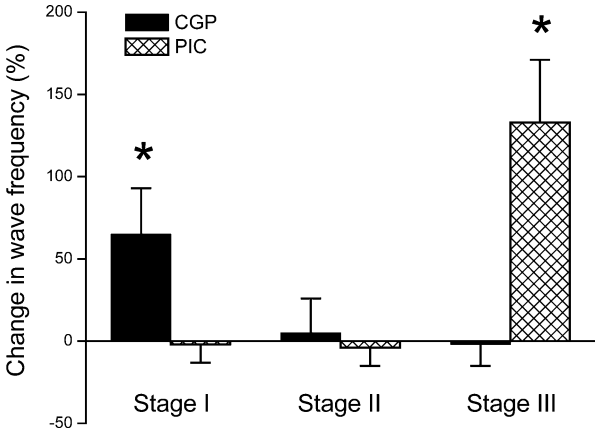

Figure 7. Developmental transition from $GABA_B$ to a $GABA_{A/C}$ modulation of retinal wave dynamics
Changes in spontaneous wave frequency (compared to control) caused by picrotoxin (PIC, 100 μM) and CGP95531 (CGP, 50 μM) are shown at three different stages. CGP significantly increased the wave frequency at stage I, but not at stage II or III, whereas PIC significantly increased wave frequency at stage III, but not at stage I or II. Asterisks indicate changes that are statistically significant ($P < 0.01$). Error bar: standard deviation.

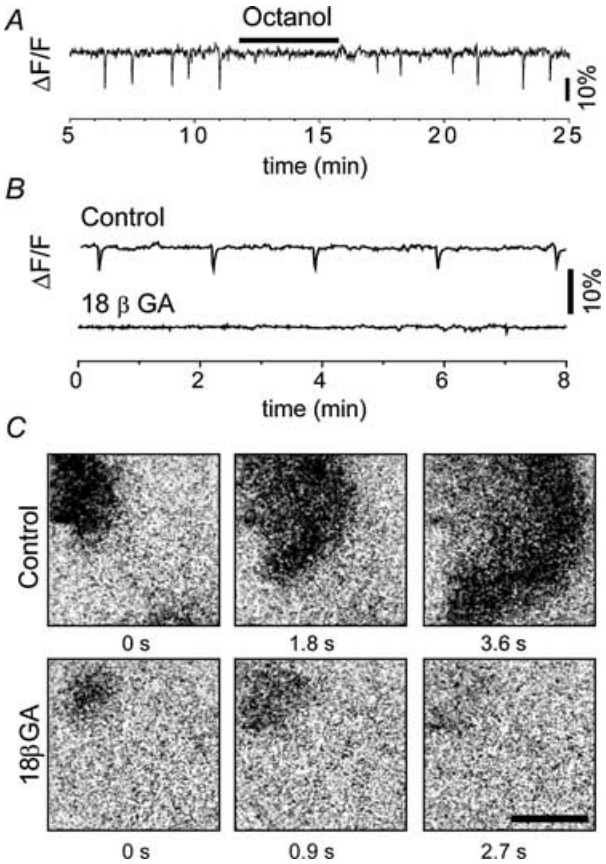

Figure 8. Effects of gap junction blockers on stage II wave
A, octanol-1 (100 μM) reversibly blocked the spontaneous waves in the ganglion cell layer of an E30 retina. *B*, waves in an E29 retina were completely blocked by 18β-GA (75 μM). *C*, a low concentration of 18β-GA (15 μM) did not completely block the wave initiation but reduced the lateral propagation of the wave at E29. Scale bar: 0.5 mm.

in the VZ and the inner retina (IR) shared a similar speed and frequency and were closely correlated in both space and time. Drugs that blocked IR waves, including hexamethonium and 18β-GA, also blocked VZ waves; however, atropine blocked only VZ, but not IR waves between E24 and P0 (stage II). We concluded that VZ waves were initiated in the IR and backpropagated to the VZ (Syed *et al.* 2004).

In this study we investigated whether VZ waves also existed at more than one developmental stage and, if so, how they progressed through various stages. We discovered that, if the retina was mounted loosely on a damp filter paper instead of a dry one, the VZ waves could be better preserved and became detectable in the same age window (E22–P8) as were IR waves, although the probability of finding VZ waves decreased considerably after P2. VZ waves could also be categorized into three stages on the basis of pharmacology. Like IR waves, stage I (E22) VZ waves were insensitive to hexamthonium (300 μM) (Fig. 9*A*, $n = 3$), but could be blocked by aminophylline (150 μM, $n = 3$) (Fig. 9*B*) and 18β-GA (75 μM, $n = 2$) (data not shown). However, in contrast to stage I IR waves which were insensitive to muscarinic antagonists (Fig. 2*A*), E22 VZ waves could be completely blocked by atropine (1 μM, $n = 2$) (Fig. 9*C*), suggesting that VZ waves required additional muscarinic communication. At stage II (P24–P1), VZ waves were inhibited by nicotinic (hexamethonium, 100 μM), muscarinic (pirenzepine, 2 μM, Fig. 9*D*-*E*) and gap junction (18β-GA, 75 μM, data not shown) blockers, but not by CNQX (40 μM) (Fig. 9*F*) or CNQX (40 μM) + AP7 (100 μM), as we previously found (Syed *et al.* 2004). At stage III (>P2), the VZ waves were blocked by CNQX (25–40 μM) + AP7 (100 μM) ($n = 3$) and the muscarinic antagonist pirenzepine (2 μM, $n = 2$) (Fig. 9*G*). We also found a transitional period between stages II and III (P2–P4), during which both hexamethonium (150 μM) and CNQX could block the VZ wave (Fig. 9*G*, $n = 2$). The nicotinic antagonist ceased to block VZ waves after P5 (Fig. 9*H*) ($n = 2$). Taken together, these data suggested that VZ and IR waves progressed through three similar developmental stages and had similar transitional periods. The main pharmacological difference between VZ and IR waves at stages I and II was that atropine blocked only VZ but not IR waves, consistent with our previous finding that stage II VZ waves are dependent on IR waves, but not *vice versa*, suggesting the waves spread from the inner to the outer retina (Syed *et al.* 2004). However, in this study, we did not investigate whether stages I and III VZ waves were correlated with IR waves in spatial and temporal domains.

Figure 10 shows examples of VZ waves at the three different stages. While stage I and stage II VZ waves were always propagating, we found most stage III VZ waves were localized, similar to their counterparts in

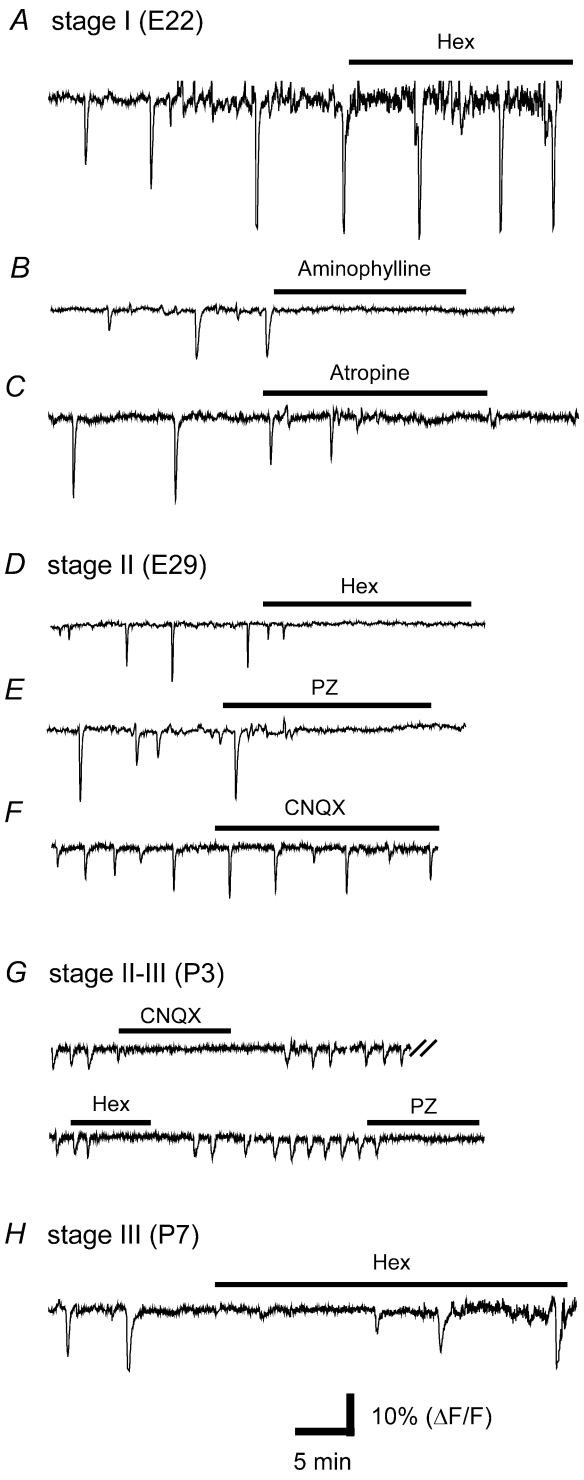

Figure 9. Three pharmacological stages of VZ waves
A–C, stage I (E22) VZ waves were not blocked by the nicotinic antagonist, haemamethonium (Hex, 300 μM), but were completely blocked by aminophylline (150 μM, *B*) and atropine (1 μM, *C*). *D–F*, stage II (E29) VZ waves could be blocked by Hex (150 μM, *D*) and the muscarinic antagonist pirenzepine (PZ, 2 μM, *E*), but not by CNQX (30 μM, *F*). *G*, At P3, the VZ waves were blocked by CNQX (30 μM), Hex (150 μM) and pirenzepine (2 μM). *H*, Hex (300 μM) no longer blocked VZ waves at P7 (stage III).

the IR. To determine whether the $GABA_{A/C}$ system also restricted the late VZ waves, we examined the effect of picrotoxin on stage II and III VZ waves. As shown in Fig. 11*A*, stage II (E30) VZ waves were not significantly affected by picrotoxin, consistent with the lack of ionotropic GABA modulation of IR waves at this stage (Fig. 5). However, the cholinesterase inhibitor, neostigmine (4 μM), which did not have a significant effect on IR waves, dramatically enhanced the amplitude and the propagation of stage II VZ waves (Fig. 11*A*) ($n = 6$), suggesting that cholinesterase activity restricted the backpropagation of the wave from IR to VZ. Interestingly, at stage III (>P2), neostigmine (4 μM) alone only slightly enhanced VZ waves (Fig. 11*B*) ($n = 4$), but application of picrotoxin (100 μM) together with neostigmine drastically enhanced both the amplitude and lateral propagation of stage III VZ waves (Fig. 11*B*) ($n = 3$), suggesting that both $GABA_{A/C}$ inhibition and cholinesterase activity reduced stage III VZ waves. Thus, endogenous ionotropic GABA inhibition played an important role in down-regulating both IR and VZ waves at stage III, although it was not clear if this inhibition downregulated VZ waves directly or mainly through an inhibition of IR waves.

Discussion

Developmental stages of spontaneous waves in the mammalian retina

The above results provide a systematic characterization of the developmental process of spontaneous waves in both the inner and outer rabbit retina, starting from the initial wave appearance prior to synaptogenesis to the final stage of spontaneous waves before eye opening. As summarized in Fig. 12, our study established three distinct developmental stages of spontaneous waves in the rabbit retina prior to eye opening. These stages coincided with three specific periods of retinal development: pre-synaptogenesis, early conventional synaptogenesis and early ribbon synaptogenesis in the IPL (McArdle *et al.* 1977; Greiner & Weidman, 1982; Robinson, 1991; Johnson *et al.* 2003). They are also consistent with the three stages of waves previously reported in the mouse retina (Bansal *et al.* 2000). More importantly, we found that each stage of wave had a distinct dynamic pattern and pharmacological profile. Stage I waves in the inner rabbit retina were novel in many aspects: they were dependent on gap junction communication but independent of nicotinic interactions; they were fast

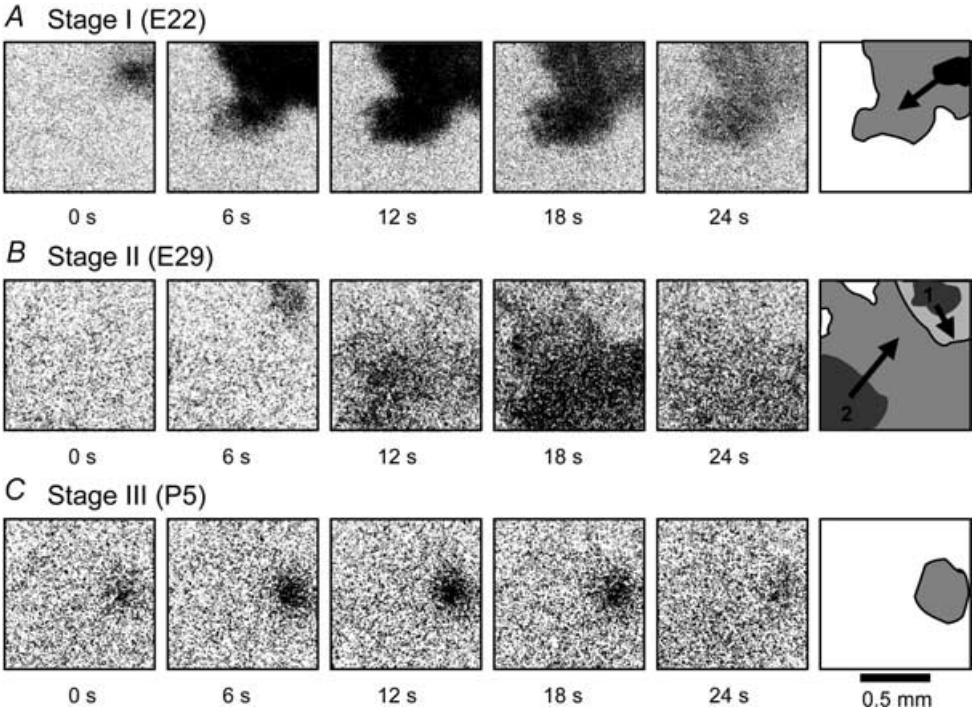

Figure 10. Stage-dependent dynamics of VZ waves
A, difference images (ΔF) of a VZ wave at E22 (stage I), showing a strong intensity (large ΔF) and clear lateral propagation of the wavefront. *B*, two stage II (E29) VZ waves forming a spatial boundary between them. *C*, a stage III (P5) VZ wave, showing a low intensity (ΔF) and localized (non-propagating) spatial pattern. The cartoon drawn in the last frame of each row shows the direction of wave propagation (arrows), the initial wave size (dark region) and the spatial coverage (grey region) of the waves.

propagating and lacked the prolonged refractory period typically found at other developmental stages; and, as a result, they appeared at a high frequency and did not observe any boundaries between neighbouring waves. The insensitivity of stage I waves to nicotinic antagonists seems to resemble the pharmacology of the localized activity previously reported in the embryonic mouse retina, where two types of spontaneous activities have been observed: non-propagating, curare-insensitive Ca^{2+} transients in small clusters of ganglion cells, and large propagating waves that were blocked by nicotinic antagonists (Bansal *et al.* 2000). It should be distinguished, however, that stage I waves in rabbit were always propagating and uniformly insensitive to nicotinic blockers. Thus, they were different from all previously reported retinal waves.

We showed that after the transition from stage I to stage II, the wave dynamics in the rabbit retina changed completely, concomitant with the emergence of the nicotinic drive for stage II waves. Remarkably, we found the transition from stage I to stage II was plastic. Blocking nicotinic receptors could revert early stage II waves back to stage I in about 15 min, indicating an ability of the network to generate more than one kind of spontaneous wave at one time. This result may explain in part why mice lacking the α_3 nAChR (nicotinic acetylcholine receptor) subunit have no stage II retinal waves but exhibit an embryonic form of patterned activity (Bansal *et al.* 2000). A similar phenomenon has also been reported in the developing spinal cord, where a blockade of one neurotransmitter system (ACh at E4, or glutamate at E11) causes a different system (GABA) to emerge as the new driving force for the spontaneous activity (Chub & O'Donovan, 1998; Milner & Landmesser,

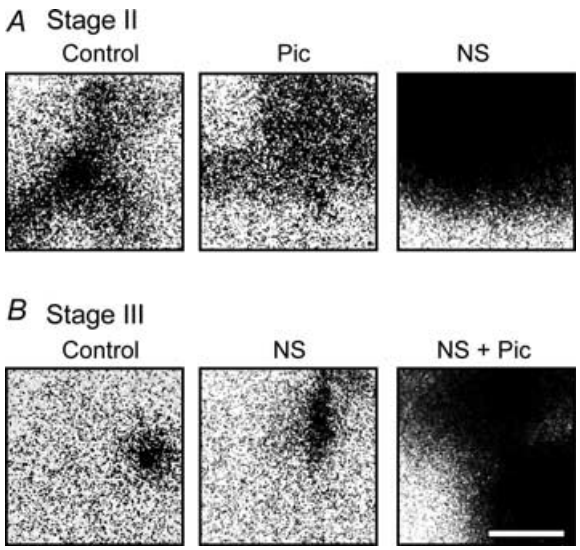

Figure 11. Modulation of VZ wave dynamics by $GABA_{A/C}$ and cholinesterase inhibitor
A, difference (ΔF) images of stage II (E30) VZ waves, showing the spatial extent of the wave (dark regions) in control, picrotoxin (Pic, 100 μM) and neostigmine (NS, 4 μM). The waves were dramatically enhanced by NS, but not by Pic at this stage. *B*, VZ waves at P3, showing a localized pattern in control, a modest enhancement in the presence of NS (4 μM) and a dramatic enhancement of wave intensity and lateral propagation in the combined presence of NS (4 μM) and Pic (100 μM). All frames were selected to show the typical wavefront size under each recording condition. Scale bar: 0.5 mm.

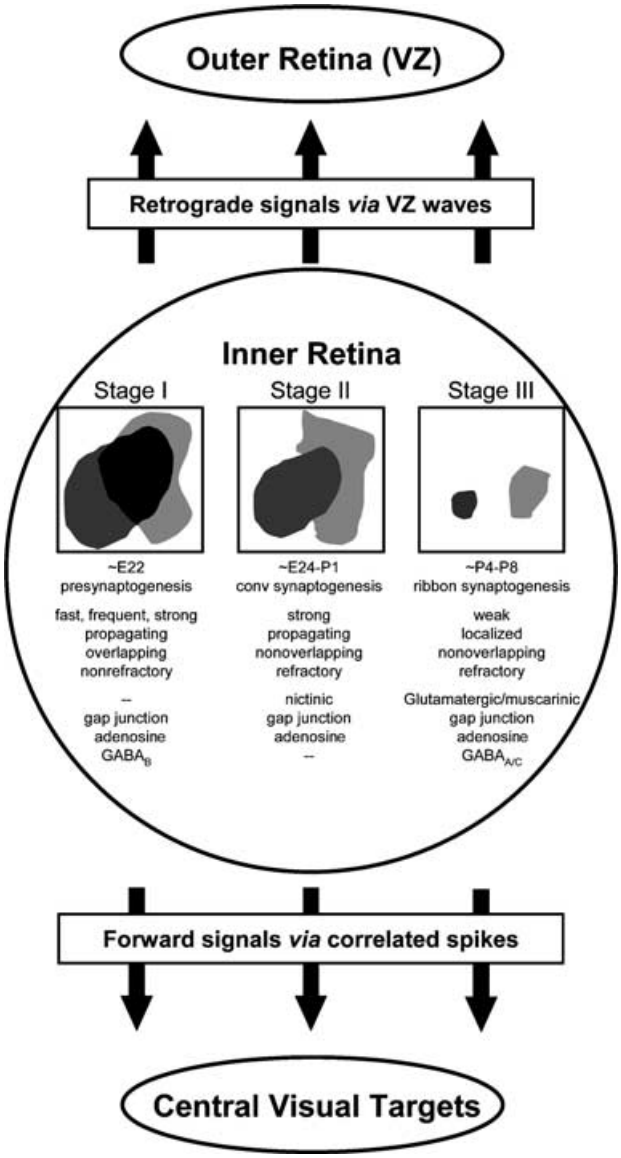

Figure 12. Developmental stages of spontaneous waves in the rabbit retina prior to eye opening
Spontaneous waves in the inner retina developed through three stages. Stage I waves were frequent, fast-propagating and non-refractory (did not form boundaries, as indicated by the overlap between two waves). They were inhibited by gap junction and adenosine receptor blockers and were downmodulated by $GABA_B$ activation. Stage II waves were propagating, refractory and non-overlapping, and were inhibited by nicotinic and gap junction blockers. Stage III waves were weak and localized. They were sensitive to glutamatergic, muscarinic and gap junction blockers, and were strongly inhibited by $GABA_{A/C}$ activation. All three stages of IR waves propagated to the outer retina (ventricular zone), thus sending both retrograde signals to the outer retina via VZ waves and forward signals to the central visual targets via correlated spikes.

1999). It has been proposed that the early spinal cord network maintains its homeostatic regulation of network firing properties by having multiple mechanisms that are capable of compensating one another when the excitability of one mechanism is reduced (O'Donovan, 1999). Our results suggest that a similar mechanism may also exist in the developing mammalian retina. However, because the waves (stage I) that reappeared 10–15 min after the blockade of the nicotinic system were dramatically different from the original (stage II) waves (Fig. 4*D*), our results also demonstrated that the coexisting mechanisms, though capable of mutual compensation, are not functionally equivalent. It should also be pointed out that the reversion of stage II waves to stage I after nicotinic blockade was rarely seen. Blocking stage II waves in E29 rabbits, for example, never resulted in an induction of stage I waves. It is thus likely that these compensatory mechanisms only coexisted during the transitional period between two different stages.

Stage III waves in the rabbit are critically dependent on glutamatergic and muscarinic inputs, but not on nicotinic excitation (Zhou & Zhao, 2000). As the retina continued to mature, stage III waves became weaker, less frequent, and spatially more restricted. They were rarely detected after P6–7. The steady decline of stage III waves with age indicated that spontaneous waves would disappear shortly after P8, probably around eye opening (P11). P8 is also the age when rabbit ganglion cells first show light responses (Masland, 1977). However, it should be noted that patch-clamp recordings occasionally found rhythmic activities from starburst and ganglion cells even after eye opening (S. Lee and J. Z. Zhou, unpublished observation). These events occurred in semi-periodic bursts at a frequency (~0.2 Hz) much higher than that of stage III waves (~0.004 Hz), but they were not observed consistently and could sometimes be disrupted by light stimulation. As the retina further matured, these events were replaced by even more frequent (nearly continuous) bursts of synaptic events (S. Lee and J. Z. Zhou, unpublished observation), suggesting that they might represent an early form of the spontaneous synaptic activity found in the mature retina, although one cannot rule out the possibility that these bursts might be considered yet another stage (stage IV) of spontaneous retinal waves, that appear around eye opening and disappear quickly thereafter. Multielectrode recordings from the GCL of the mouse retina found rhythmic activities around eye opening that were temporally correlated (Demas *et al.* 2003).

Stage-dependent GABAergic modulation of retinal waves

Our results demonstrated an important role of GABA in regulating the dynamics of mammalian retinal waves, consistent with previous reports in lower vertebrates that $GABA_B$ activation modulates retinal waves in the early chick (Catsicas & Mobbs, 2001) and $GABA_A$ activation modulates retinal waves in the turtle (Sernagor *et al.* 2003*b*). Importantly, we showed that the GABAergic regulation of retinal wave dynamics was stage dependent, involving an interesting transition from a $GABA_B$ to a $GABA_{A/C}$ system as development proceeded from stage I to stage III. By using two different families of receptors for the same transmitter, the GABAergic system was able to achieve different levels of regulation at different stages. This is reminiscent of the stage-dependent involvement of the nicotinic (at stage II) and muscarinic (at stage III) systems in the generation of the IR waves in rabbit (Zhou & Zhao, 2000).

Because the early-developing neural network is highly excitable due to the early excitatory actions of GABA and glycine receptor channels (Ben-Ari, 2002), the regulation of spontaneous bursts of excitation in many early-developing networks is thought to be mediated by homeostasis (O'Donovan, 1999). Our finding of the GABAergic inhibition of retinal waves now suggests that neurotransmitter-mediated inhibition also plays an important role in regulating the pattern of early spontaneous retinal waves. This inhibition may be particularly important for stage I waves, since these waves did not have a prolonged postwave refractory period. Although the cellular mechanism of the $GABA_B$ modulation of stage I waves in the rabbit remains to be uncovered, it seems that the cyclic AMP pathway is likely to be involved (Catsicas & Mobbs, 2001), since activating adenylate cyclase with forskolin enhanced the wave tremendously (Fig. 2). Thus, the adenosine (probably via A2 receptors) and $GABA_B$ systems may act in opposition to regulate the wave dynamics at this early stage of development.

Our result that $GABA_{A/C}$ antagonists dramatically increased the amplitude, frequency, speed and lateral propagation of stage III waves and induced propagating waves in older (>P6) retinas that did not show spontaneous waves suggests an important role of the $GABA_{A/C}$-mediated inhibition in the decline and eventual disappearance of stage III retinal waves. This conclusion is also consistent with a similar finding in the turtle retina (Sernagor *et al.* 2003*b*). While our results clearly demonstrated a role of the GABAergic system in shaping the wave dynamics at stage I and stage III, it is currently unclear and puzzling why blocking endogenous GABA transmission (both $GABA_{A/C}$ and $GABA_B$) apparently did not affect the wave dynamics at stage II (Fig. 3*B*), even though patch-clamp recordings from rabbit starburst amacrine and ganglion cells showed robust $GABA_A$ inputs to these cells during the wave (S. Lee and Z. J. Zhou, unpublished observation). Application of picrotoxin to the ferret retina at a similar stage also did not result

in a detectable change in wave dynamics (Stellwagen *et al.* 1999). Interestingly, a recent report in the turtle (Sernagor *et al.* 2003*a*) suggests that GABA input during spontaneous waves may be important for the expression of the K^+–Cl^- cotransporter, KCC2. Thus, it is possible that the GABA input during stage II waves may be critical for the development of $GABA_{A/C}$ inhibition at stage III, even though GABA does not affect the wave dynamics at stage II.

Spontaneous waves existed over an extensive developmental period and appeared in more than one retinal layer

It has been previously reported that spontaneous retinal activity plays a critical role in the refinement of retinogeniculate and retinocollicular connectivity (Penn *et al.* 1998; Stellwagen & Shatz, 2002; Grubb *et al.* 2003; McLaughlin *et al.* 2003), although the exact function of the waves in retinogenicular development remains controversial (Huberman *et al.* 2003). Our observation of both VZ and IR waves at all three stages of wave development suggests that rhythmic spontaneous retinal activity is a general developmental phenomenon that is not limited to a single critical period or a single developmental event. The first appearance of the waves at E22 closely correlates in time with the initial arrival of ganglion cell axon terminals at the central visual targets (Crabtree, 1989, 1990; Gayer *et al.* 1989). Our results show that spontaneous retinal waves are present and may play a role during the entire developmental period of retinogenicular and retinocollicular projections prior to eye opening. Thus, in the case of the developmental sequence of retinogenculate projections, stage I waves correspond to the initial innervation of optic nerve at the dLGN; stage II waves occurred during both the initial establishment of overlapping contra- and ipsilateral retinogeneculate connectivity and the subsequent refinement into eye-specific segregation in the alpha sector of the dLGN, which becomes nearly adult-like at E29–P3 (Gayer *et al.* 1989; Crabtree, 1990); and stage III waves may correspond to a period of more advanced connectivity refinement in the dLGN, such as ON/OFF segregation (Wong, 1999).

The presence of waves in both the inner and outer retina indicates that the waves are a property of both differentiated and undifferentiated/differentiating cells. Thus the developmental function of retinal waves is likely to be diverse, involving not only the establishment of precise retinofugal projections, but also the development of the retina itself, such as retinal cell cycle (Pearson *et al.* 2002) and receptive field formation (Sernagor & Grzywacz, 1996). As retinal waves progress from one stage to another (Fig. 12), their functional role will also evolve. Since the spatiotemporal pattern of spontaneous activity is thought to be important in encoding certain developmental cues (Spitzer & Gu, 1997), it seems natural that the wave dynamics are regulated differently at each stage for specific functions. We showed that different neurotransmitter systems shape the wave dynamics at different stages. Conversely, one may speculate that the normal development of these transmitter systems may in turn rely on the cues provided by the wave in a stage-specific manner. A full appreciation of the developmental functions of retinal waves would require the understanding of the complex developmental process and regulation of the waves.

References

Ames A & Nesbett FB (1981). In vitro retina as an experimental model of the central nervous system. *J Neurochem* **37**, 867–877.

Bansal A, Singer JH, Hwang BJ, Xu W, Beaudet A & Feller MB (2000). Mice lacking specific nicotinic acetylcholine receptor subunits exhibit dramatically altered spontaneous activity patterns and reveal a limited role for retinal waves in forming ON and OFF circuits in the inner retina. *J Neurosci* **20**, 7672–7681.

Ben-Ari Y (2002). Excitatory actions of GABA during development: the nature of the nurture. *Nat Rev Neurosci* **3**, 728–739.

Burnstock G & Williams M (2000). P2 purinergic receptors: modulation of cell function and therapeutic potential. *J Pharmacol Exp Ther* **295**, 862–869.

Catsicas M, Bonness V, Becker D & Mobbs P (1998). Spontaneous Ca^{2+} transients and their transmission in the developing chick retina. *Curr Biol* **8**, 283–286.

Catsicas M & Mobbs P (2001). $GABA_B$ receptors regulate chick retinal calcium waves. *J Neurosci* **21**, 897–910.

Chub N & O'Donovan MJ (1998). Blockade and recovery of spontaneous rhythmic activity after application of neurotransmitter antagonists to spinal networks of the chick embryo. *J Neurosci* **18**, 294–306.

Crabtree JW (1989). Prenatal development of retinocollicular projections in the rabbit: an HRP study. *J Comp Neurol* **286**, 504–513.

Crabtree JW (1990). Prenatal development of retinogeniculate projections in the rabbit: an HRP study. *J Comp Neurol* **299**, 75–88.

Demas J, Eglen SJ & Wong RO (2003). Developmental loss of synchronous spontaneous activity in the mouse retina is independent of visual experience. *J Neurosci* **23**, 2851–2860.

Feller MB (1999). Spontaneous correlated activity in developing neural circuits. *Neuron* **22**, 653–656.

Feller MB, Butts DA, Aaron HL, Rokhsar DS & Shatz CJ (1997). Dynamic processes shape spatiotemporal properties of retinal waves. *Neuron* **19**, 293–306.

Feller MB, Wellis DP, Stellwagen D, Werblin FS & Shatz CJ (1996). Requirement for cholinergic synaptic transmission in the propagation of spontaneous retinal waves. *Science* **272**, 1182–1187.

Gayer NS, Horsburgh GM & Dreher B (1989). Developmental changes in the pattern of retinal projections in pigmented and albino rabbits. *Brain Res Dev Brain Res* **50**, 33–54.

Greiner JV & Weidman TA (1982). Embryogenesis of the rabbit retina. *Exp Eye Res* **34**, 749–765.

Grubb MS, Rossi FM, Changeux JP & Thompson ID (2003). Abnormal functional organization in the dorsal lateral geniculate nucleus of mice lacking the beta 2 subunit of the nicotinic acetylcholine receptor. *Neuron* **40**, 1161–1172.

Huberman AD, Wang GY, Liets LC, Collins OA, Chapman B & Chalupa LM (2003). Eye-specific retinogeniculate segregation independent of normal neuronal activity. *Science* **300**, 994–998.

Johnson J, Tian N, Caywood MS, Reimer RJ, Edwards RH & Copenhagen DR (2003). Vesicular neurotransmitter transporter expression in developing postnatal rodent retina: GABA and glycine precede glutamate. *J Neurosci* **23**, 518–529.

Katz LC & Shatz CJ (1996). Synaptic activity and the construction of cortical circuits. *Science* **274**, 1133–1138.

Maffei L & Galli-Resta L (1990). Correlation in the discharges of neighboring rat retinal ganglion cells during prenatal life. *Proc Natl Acad Sci U S A* **87**, 2861–2864.

Masland RH (1977). Maturation of function in the developing rabbit retina. *J Comp Neurol* **175**, 275–286.

McArdle CB, Dowling JE & Masland RH (1977). Development of outer segments and synapses in the rabbit retina. *J Comp Neurol* **175**, 253–274.

McLaughlin T, Torborg CL, Feller MB & O'Leary DD (2003). Retinotopic map refinement requires spontaneous retinal waves during a brief critical period of development. *Neuron* **40**, 1147–1160.

Meister M, Wong RO, Baylor DA & Shatz CJ (1991). Synchronous bursts of action potentials in ganglion cells of the developing mammalian retina. *Science* **252**, 939–943.

Milner LD & Landmesser LT (1999). Cholinergic and GABAergic inputs drive patterned spontaneous motoneuron activity before target contact. *J Neurosci* **19**, 3007–3022.

Norenberg W & Illes P (2000). Neuronal P2X receptors: localisation and functional properties. *Naunyn Schmiedebergs Arch Pharmacol* **362**, 324–339.

O'Donovan MJ (1999). The origin of spontaneous activity in developing networks of the vertebrate nervous system. *Curr Opin Neurobiol* **9**, 94–104.

Pearson R, Catsicas M, Becker D & Mobbs P (2002). Purinergic and muscarinic modulation of the cell cycle and calcium signaling in the chick retinal ventricular zone. *J Neurosci* **22**, 7569–7579.

Penn AA, Riquelme PA, Feller MB & Shatz CJ (1998). Competition in retinogeniculate patterning driven by spontaneous activity. *Science* **279**, 2108–2112.

Robinson SR (1991). Development of the mammalian retina. In *Vision and Visual Dysfunction*, vol. 3, ed. Cronly-Dillon JR, pp. 69–138. Macmillan, London.

Sernagor E & Grzywacz NM (1996). Influence of spontaneous activity and visual experience on developing retinal receptive fields. *Curr Biol* **6**, 1503–1508.

Sernagor E, Lectch C, Young V & Metha V (2003*a*). Developmental changes in $GABA_A$ receptor-driven activity mediate the maturation of retinal spontaneous activity patterns. 2003 Abstract Viewer/Itinerary Planner. Washington, DC. Society for Neuroscience. Program no. 655.4, Online.

Sernagor E, Young C & Eglen SJ (2003*b*). Developmental modulation of retinal wave dynamics: shedding light on the GABA saga. *J Neurosci* **23**, 7621–7629.

Spitzer NC & Gu X (1997). Purposeful patterns of spontaneous calcium transients in embryonic spinal neurons. *Semin Cell Dev Biol* **8**, 13–19.

Stellwagen D & Shatz CJ (2002). An instructive role for retinal waves in the development of retinogeniculate connectivity. *Neuron* **33**, 357–367.

Stellwagen D, Shatz CJ & Feller MB (1999). Dynamics of retinal waves are controlled by cyclic AMP. *Neuron* **24**, 673–685.

Syed MM, Lee S, He S & Zhou ZJ (2004). Spontaneous waves in the ventricular zone of developing mammalian retina. *J Neurophysiol* **91**, 1999–2009.

von Kugelgen I & Wetter A (2000). Molecular pharmacology of P2Y-receptors. *Naunyn Schmiedebergs Arch Pharmacol* **362**, 310–323.

Vu TQ, Payne JA & Copenhagen DR (2000). Localization and developmental expression patterns of the neuronal K-Cl cotransporter (KCC2) in the rat retina. *J Neurosci* **20**, 1414–1423.

Wong RO (1999). Retinal waves and visual system development. *Annu Rev Neurosci* **22**, 29–47.

Wong RO & Oakley DM (1996). Changing patterns of spontaneous bursting activity of on and off retinal ganglion cells during development. *Neuron* **16**, 1087–1095.

Wong WT, Myhr KL, Miller ED & Wong RO (2000). Developmental changes in the neurotransmitter regulation of correlated spontaneous retinal activity. *J Neurosci* **20**, 351–360.

Zhao D, Cornett L & Zhou ZJ (1999). Consistency and modulation of spontaneous waves of excitation in the developing rabbit retina. *Abstracts: Soc Neurosci* **25**, 1807.

Zhou ZJ (1998). Direct participation of starburst amacrine cells in spontaneous rhythmic activities in the developing mammalian retina. *J Neurosci* **18**, 4155–4165.

Zhou ZJ (2001). A critical role of the strychnine-sensitive glycinergic system in spontaneous retinal waves of the developing rabbit. *J Neurosci* **21**, 5158–5168.

Zhou ZJ, Lee S & Syed MM (2002). Multistage and multidimensional retinal waves suggest diverse developmental roles. *2002 Abstract Viewer/Itinerary Planner. Washington, DC. Society for Neuroscience*. Program no. 236.1, Online.

Zhou ZJ & Zhao D (2000). Coordinated transitions in neurotransmitter systems for the initiation and propagation of spontaneous retinal waves. *J Neurosci* **20**, 6570–6577.

Acknowledgements

We thank James McCarley, Dichen Zhao and Qing Yang for help with some of the experiments. This work was supported in part by a grant from NIH (EY10894 to ZJZ) and by unrestricted grants from Research to Prevent Blindness and the Pat and Willard Walker Eye Research Center.

Supplementary material

The online version of this paper can be accessed at:
DOI: 10.1113/jphysiol.2004.066597
http://jp.physoc.org/cgi/content/full/jphysiol.2004.066597/DC1

and contains supplementary material consisting of movies (AVI format) of spontaneous stage I, II and III waves in the ganglion cell layer of Fura-2AM-loaded retinas from E22, E29 and P5 rabbits, respectively. The images in the movies were subtracted by a control image acquired prior to a spontaneous wave and represent difference fluorescence images ($\triangle F$). Darker regions in the images correspond to increases in calcium concentration. The movies are played at 9× the real speed. Frame size: 1.14 mm × 1.14 mm. Representative frames from these movies are also shown in parts of Fig. 3 in this paper.
This material can also be found at:
http://www.blackwellpublishing.com/products/journals/suppmat/tjp/tjp496/tjp496sm.htm